



HAL
open science

Designing a multi-channel 47 GHz microwave diagnostic for plasma edge measurements

H Faugel, M Usoltseva, Stéphane Heuraux, V Bobkov, Asdex Upgrade Team

► **To cite this version:**

H Faugel, M Usoltseva, Stéphane Heuraux, V Bobkov, Asdex Upgrade Team. Designing a multi-channel 47 GHz microwave diagnostic for plasma edge measurements. 24th Topical conference on radio-frequency power in plasmas, Sep 2022, Annapolis, United States. pp.110004, 10.1063/5.0162547. hal-04190613

HAL Id: hal-04190613

<https://hal.univ-lorraine.fr/hal-04190613>

Submitted on 29 Aug 2023

HAL is a multi-disciplinary open access archive for the deposit and dissemination of scientific research documents, whether they are published or not. The documents may come from teaching and research institutions in France or abroad, or from public or private research centers.

L'archive ouverte pluridisciplinaire **HAL**, est destinée au dépôt et à la diffusion de documents scientifiques de niveau recherche, publiés ou non, émanant des établissements d'enseignement et de recherche français ou étrangers, des laboratoires publics ou privés.



Distributed under a Creative Commons Attribution 4.0 International License

Designing a Multi-Channel 47 GHz Microwave Diagnostic for Plasma Edge Measurements

H. Fauge^{1 a}, M. Usoltseva¹, S. Heurax², V. Bobkov¹, ASDEX Upgrade Team¹

¹Max Planck Institute for Plasma Physics, Boltzmannstraße 2, 85748 Garching, Germany

²Université de Lorraine-CNRS, Institut Jean Lamour, BP50840, F-54011 Nancy, France

^a Corresponding author: helmut.faugel@ipp.mpg.de

Abstract. The measurement of the plasma parameters close to the ICRF antennas is important to understand the wave propagation and improve modelling. For this purpose one of the 3-strap ICRF antennas in ASDEX Upgrade, that were installed in 2014, is equipped with 10 horn antenna pairs; three of these antenna pairs are used for reflectometry in the extended U-Band at frequencies from 40 – 68 GHz. One of the unused horn antenna pairs close to the ICRF antenna limiter was removed; with some additional waveguide sections and new supports for the horn antennas we could set up a new microwave diagnostic that allows density measurements in the limiter shadow. The diagnostic, called Microwave Intensity refractometer in the Limiter Shadow (MILS), operates with 47 GHz amateur radio transmitter and receiver units and allows phase and amplitude measurements at an intermediate frequency of 145 MHz. After the successful installation and commissioning of MILS in 2019 and some modifications in 2020, we plan to upgrade the system to three receiver horn antennas, as the microwave beam from the transmitter horn antenna, which is tangential to the plasma, is refracted by the large density gradient at the plasma edge. The amplitude and phase information from the addition receiver antennas will improve our knowledge about the plasma properties.

INTRODUCTION

The same hardware, as was already used in the IShTAR teststand to perform a density measurement of the helicon discharges, was implemented for density measurements at the plasma edge in the ASDEX Upgrade tokamak. After a number of improvements of in vessel installations, phase detectors and data acquisition the diagnostic became very reliable. Data analysis techniques have been developed [1, 2] and the measured density has been benchmarked to other diagnostics [3]. The diagnostic physical principle is different from the existing techniques of microwave interferometry and reflectometry, therefore a new term “intensity refractometry” was introduced for this technique [3]. In parallel modelling of the plasma edge and ray tracing of the microwave beam showed the potential use additional receiving horn antennas.

MEASUREMENT SETUP

In order to roughly estimate the needed diagnostic parameters, the measurement principle of a microwave interferometer was used to predict the range of measured values. In an interferometer, the change of phase velocity is caused by the electron density along the microwave beam. As long as the operation frequency is below the cutoff density, a measurement of the phase shift allows an integral density measurement along the microwave beam. As the interferometer should be able to measure densities above from 10^{16} m^{-3} and we wanted to use some already installed U-band waveguides (WR 19, frequency range 40 – 60 GHz) and horn antennas which have an opening of 20 x 27 mm, with a radiation angle of $\pm 8.25^\circ$. We decided to use readily available amateur radio electronics operating at 47.088 – 47.090 GHz; the cutoff density at that frequency is $2.8 \times 10^{19} \text{ m}^{-3}$ which is well above the density we expect

at the plasma edge. The distance of the two horn antennas was 429.6 mm, a distance of 25 mm behind the limiters of the ICRF antenna had to be maintained for machine safety.

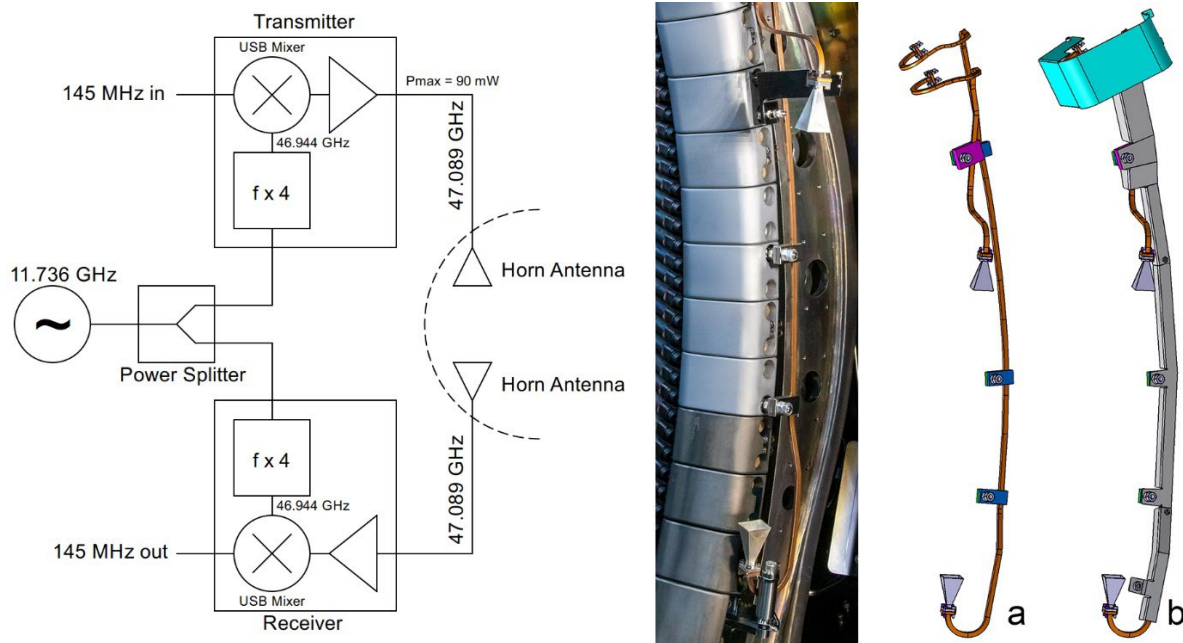


FIGURE 1. Block diagram of the MILS diagnostic (left). The diagnostic is operated a 145 MHz, both transmitter and receiver need a local oscillator at 11.736 GHz, which is internally multiplied by 4 giving 46.944 GHz. A single side mixer converts the 145 MHz input signal to the upper side band (USB) at 47.089 GHz. The maximum output power of the transmitter is 90 mW, the attenuation of the waveguide, 1.2 dB/m, reduces the power at the horn antenna to about 10 mW. The received signal is amplified and down converted to 145 MHz; as both transmitter and receiver use the same local oscillator signal the received signal is phase locked, allowing measuring the phase change caused by the plasma. The picture shows the installation in the vessel attached to the ICRF antenna 4, distance of the horn antennas is 430 mm. The CAD drawing (a) shows the installed MILS setup in 2019. In 2020, stainless steel heat shields were added to reduce the thermal expansion of the waveguides (b).

We decided to use two Kuhne MKU 47 G2 transverter modules [4], one configured as transmitter, the other as receiver as the main microwave components of MILS. The recommended reference oscillator is the Kuhne MKU LO 8-13 PLL [5], which provides a local oscillator signal of 11.736 GHz. This frequency is internally multiplied by four in the receiver and transmitter; giving 46.944 GHz. Furthermore, an intermediate frequency (IF) source between 144 – 146 MHz for the upper sideband image rejection mixer of transmitter is required. Using the middle of the IF-band at 145 MHz results in an operating frequency of 47.089 GHz of MILS. As receiver and transmitter use the same local oscillator signal, splitted by a power splitter, the whole system is coherent and permits phase detection at the intermediate frequency at 145 MHz. A phase detector, similar to the models being used for the ICRF and plasma density diagnostic [6] is used to measure the phase difference between the reference signal and the received signal.

DEBUGGING THE ORIGINAL INSTALLATION

The original MILS diagnostic was built at a very tight time frame of only five months from the basic idea till finishing in vessel installation. As the Reflectometer in the ICRF antenna diagnostic [7] had a number of spare waveguides we decided the use two of these waveguides for the MILS. This required the design of supports for the horn antennas and additional waveguides inside vessel, in the experiment hall addition waveguides, microwave electronics and cables to an already existing data acquisition were installed.

The data of the first measurements confirmed the measurement principle, showing changes in amplitude and phase compared during the plasma discharges. Not very surprisingly, the operation had from time to time some issues. The first thing we noted was a loss of the received signal at certain plasma configurations. After contacting the manufacturer of the microwave electronics, we concluded that the local stray magnetic field causes the DC-DC converters of the electronic to turn off. The manufacturer offered a modification of the electronics with bypassing the

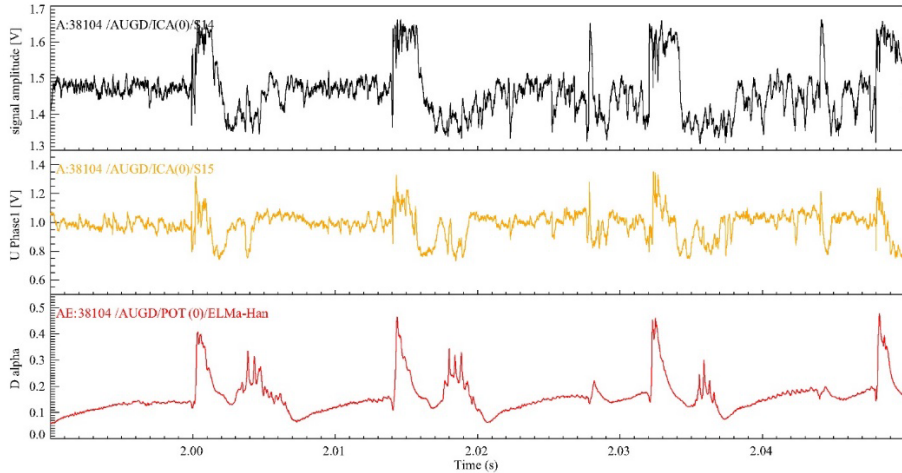


FIGURE 2. Amplitude and phase measurement during a plasma discharge with ELMs. The scaling for the amplitude is 50 mV/dB and 10 mV/° for the phase. One can clearly see that the emission of D alpha light, which mirrors quantitatively the ELM activity, and the changes in phase and amplitude correlate

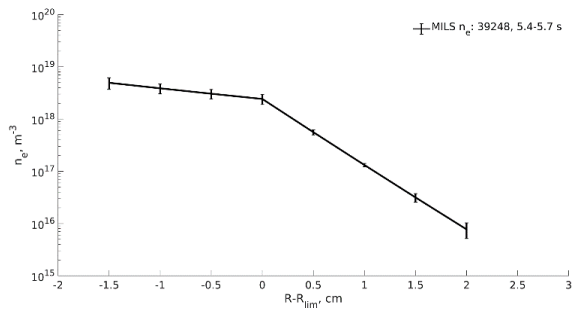
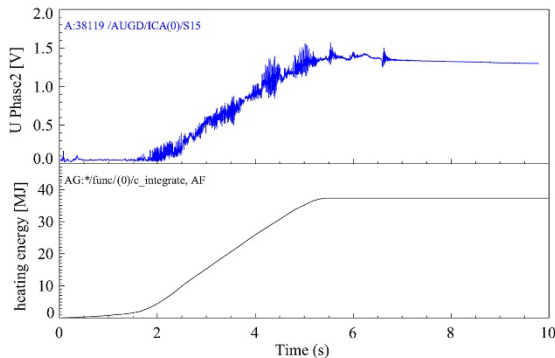


FIGURE 3. A reconstructed radial density profile the limiter using the measurements of the MILS diagnostic. The technique is presented in [6], the assumption is that the density profile consists out of two exponential functions with a transition at the limiter.



DC-DC converters, which changed the needed power supply voltage from + 12 V to + 5.2 V. This increased the reliability by a large portion.

After an analysis of the phase information, we discovered that the radiation of the plasma, which can reach values of up to 250 kW/m², heats up the waveguides causing a significant phase shift due to thermal expansion. In total about 1.95 m waveguide was exposed to plasma radiation. With a total heating energy up to 81.3 MJ per discharge, the phase shifts of up to 176.6 ° during the plasma discharge. As the wavelength in the waveguide is 4.745 mm at 47.089 GHz this is equal to 2.33 mm length increase, which is an averaged temperature increase of 72.4 K of the waveguides that are expose to the radiation from the plasma. To reduce this, we installed a sheet metal cover that shields about 80 % of exposed waveguides.

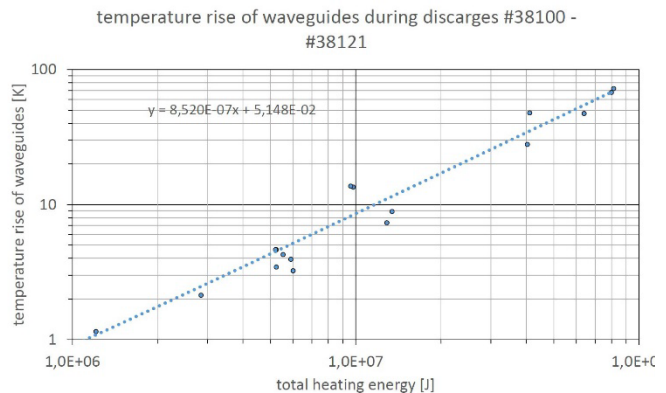


FIGURE 4. The top signal in plot on the left shows one of the phase signal during a plasma discharge. As the radiation heated the uncovered waveguides the phase changed because of thermal expansion. The curve correlates with the applied heating energy during the discharge. The left plot shows the calculated temperature rise of the waveguides as a function heating energy for a series of shots. After covering about 80 % of the waveguides with a stainless steel shield the radiation induced phase shift was halved.

As the data acquisition system of the diagnostic was shared with the retarding field analyzer (RFA) several meters away, we had to use isolation amplifiers to protect the inputs of the analog-to-digital converters (ADC). Unfortunately they not only reduced the bandwidth of the signals to 100 kHz, there as the sampling frequency of the ADCs was 2 MHz, they also introduced offset and noise. We finally installed a separate data acquisition for the MILS diagnostic, where we again had problems with tripping of switch mode power supplies after severe disruptions. Also one channel of the SIGLENT SDG6022X signal generator that provides the 145 MHz IF signals tripped at certain plasma configurations with very high currents in the vertical field coils V3 of ASDEX Upgrade. In the future, the signal generator will be replaced with a 145 MHz quartz oscillator that is not sensitive to magnetic fields.

Full-wave simulations of the microwave propagation with a modelled plasma showed that tilting the transmitter horn antenna by 10° is advantageous. These modifications were done in the 2020 opening with some further improvements in the 2021 opening. Also a cumulative reduction of about 3 dB the received signal was noted during the campaigns, while the reason for this remained unknown, in the 2022 campaign the signal reduction was much more severe.

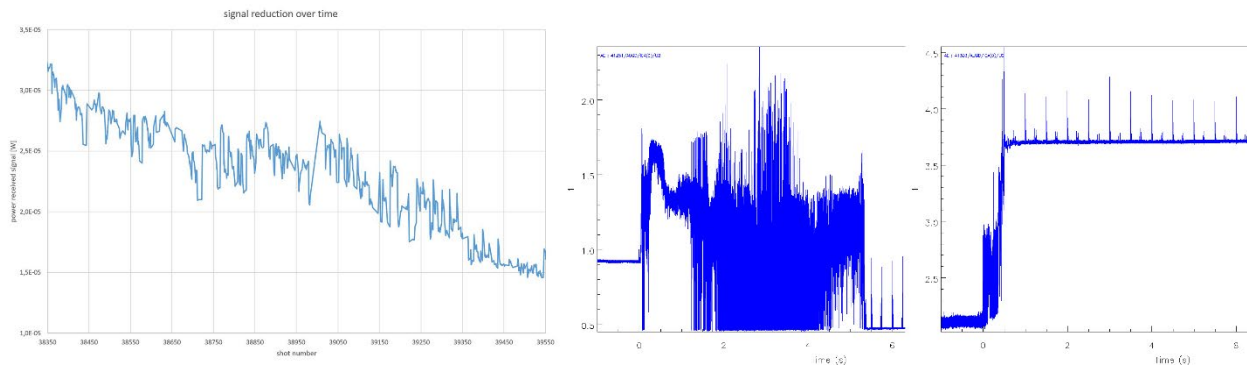


FIGURE 5. The left plot shows the reduction of received signal strength during the ASDEX Upgrade 2020 campaign. It is believed that the accumulation of dust and metallic particles on the Kapton foil between transmitter horn antenna and waveguide cause an attenuation of the signal. During a series of discharges with the boron dropper we noted a very significant reduction of the receiver signal from shot to shot. During ramp down of the plasma shot # 41251 the signal finally vanished (central plot). Adding a 40 dB amplifier in the receiver path brought the signal level back into the detection range. During the startup of shot #41303 the blocking of the antenna disappeared causing a signal increase of 32 dB, almost overdriving the detector (right plot).

As we installed a $25\ \mu\text{m}$ thick Kapton foil (with a central 1.5 mm hole for outgassing of the waveguide) between the flanges of the upward pointing transmitter horn antenna and the waveguide we suspected dust accumulation or thin layers deposited during boronisation of the vessel. After checking the data, we could exclude the boronisations, but changes up to 25 dB attenuation from shot to shot were observed. Studying literature [8] pointed us to the fact that even very thin metallic layers can cause high attenuation. An inspection in the 2022 open showed a shiny metallic surface on the Kapton foil.

MEASURING MICROWAVE EMISSION FROM THE PLASMA

Once we faced a trip of our 145 MHz signal generator, which led to the case that MILS did not transmit a signal. As the receiver was still active, we were able to measure the microwave emission from the plasma edge. The signal levels is quite weak reaching up to $-30\ \text{dBm}$ at the rf detector, which is well within the range of the logarithmic rf detector. As the receiver has 37 dB gain, and the attenuation of the waveguide to the antenna is 10 dB, the antenna picks up around $-57\ \text{dBm}$ of noise over the receiver bandwidth. Assuming a receiver bandwidth of 20 MHz the noise density is up to $10^{-16}\ \text{W/Hz}$.

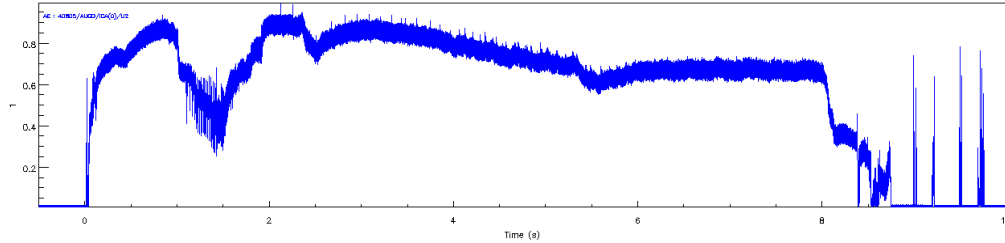


FIGURE 6. Measured microwave emission at plasma edge during a shot. At 8 s the plasma is ramped down, the peaks after 8.5 s are believed to be spurious pickups from the still running Doppler-reflectometer.

PHASE DETECTORS

The phase detector used for the MILS was basically a modified one from the ICRF, however as it had to work at 145 MHz instead of 30 – 60 MHz some changes were necessary, e.g. removing of the switchable 50 and 90 MHz low pass filters and the 90 ° power splitter was replaced with a type working at 145 MHz. A bit surprisingly, the isolation between the reference and received signal was only 35 dB, which causes a phase error of up to $\pm 1^\circ$ if both signals have the same amplitude. A revised printed circuit board did not improve the isolation; therefore, we tried a different approach where we down converted the 145 MHz signals to 5 MHz. The idea was to perform the phase detection with a dedicated phase detector ICs like the AD9901 or the 74HC297. It turned out that both ICs had issues making them useless for phase measurement purposes. An attempt using standard CMOS gates for phase detection could track the phase shifts over more than 360° without any uncertainty. However, for small phase changes the characteristic showed non-linearities caused by the gate delay times and the ringing of the output signals, an appropriate calibration table would have been extensive. A phase detector with two analog multipliers AD831 delivering in-phase and quadrature components (I and Q signals) was developed, which is currently manufactured. Extensive simulation with LTSpice using e.g. a model of the analog multiplier allowed a detailed analysis of the dynamic behavior, furthermore the analysis of the influence of harmonics present at the inputs led to a redesign of the needed filtering

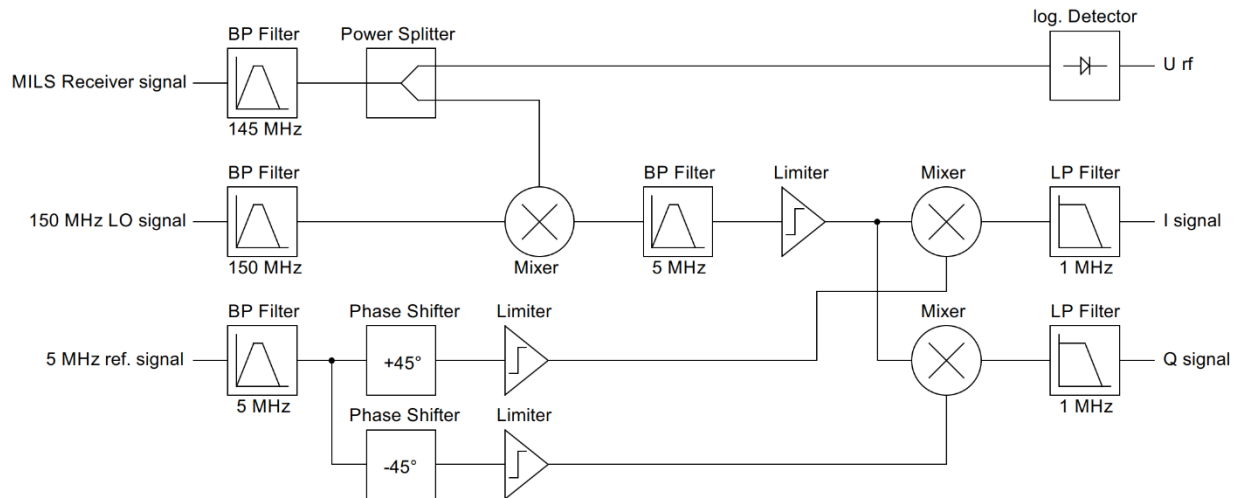


FIGURE 7. Block diagram of the latest phase detector design. The received signal is splitted, one signal is feed in logarithmic power detector and the other signal is down converted to 5 MHz with a 150 MHz local oscillator. A 5 MHz reference signal that is derived from the 145 MHz transmitter signal and the 150 MHz local oscillator is shifted by $+45^\circ$ respectively -45° in order to provide signals with 90° phase shift for quadrature demodulation of the received signal. The limiter amplifiers provide constant amplitudes at the mixer inputs; as both inputs at the mixers have the same frequency, the output signal consists of a DC voltage and a signal of the double input frequency. The low pass filters remove the rf components of the signal, a bandwidth of 1 MHz is sufficient for the data acquisition operating with 2 MHz sample frequency.

ADDING MORE RECEIVER CHANNELS

Raytracing and the full-wave modelling of the transmitted microwave beam showed, that due to refraction, the beam is diverged over a large width, which cannot be covered with a single receiver horn antenna. As there are unused waveguides from the ICRF antenna reflectometer available, we plan to add two additional horn antennas forming an array of three antennas. Modelling shows what could be achieved with such a configuration. The design is not finalized yet; we plan to realize this project with the colleagues from the IGVP of the University of Stuttgart, as they have extensive knowledge in designing and manufacturing of microwave components, e.g. ECRH launchers etc.

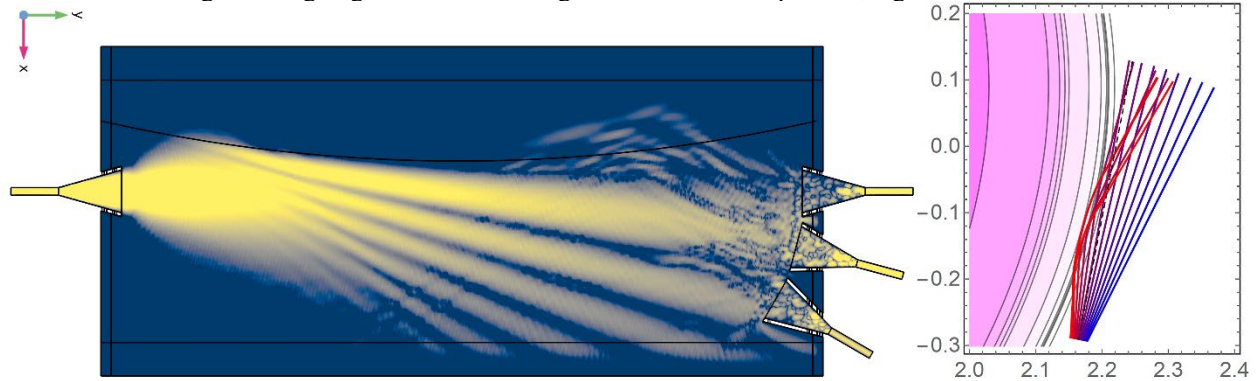


FIGURE 8. Raytraced microwave beam along the plasma edge. Left picture: the beam is launched with a horn antenna on the left side, is partly refracted by the plasma (downward curved black line) and is received by three horn antennas. The right plot shows how the microwave beam is refracted at the plasma edge, note the bending of the reddish rays, which overlap with other rays.

ACKNOWLEDGMENTS

The authors would like to thank Gerhard Siegl and Johann Kneidl for the installation of the diagnostic in the vessel, Andreas Wöls for helping out with spare power supplies and Hans Huber for assembling the printed circuits boards of the phase detectors, Dietmar Wagner calculated the effects of thin metal apertures in waveguides.

This work has been carried out within the framework of the EUROfusion Consortium, funded by the European Union via the Euratom Research and Training Programme (Grant Agreement No 101052200 — EUROfusion). Views and opinions expressed are however those of the author(s) only and do not necessarily reflect those of the European Union or the European Commission. Neither the European Union nor the European Commission can be held responsible for them.

REFERENCES

1. M. Usoltceva, S. Heurax, I. Khabibullin and H. Faugel, *Rev. Sci. Instrum.* **93**, 013502 (2022) doi:[10.1002/ctpp.202100194](https://doi.org/10.1002/ctpp.202100194)
2. M. Usoltceva et al., *Fusion Eng. Des.* **165**, 112269 (2021) doi: [10.1063/5.0074838](https://doi.org/10.1063/5.0074838)
3. M. Usoltceva et al., “Experimental validation of the intensity refractometry principle for density measurements at the edge of a tokamak”, submitted to *Rev. Sci. Instrum.*
4. <https://shop.kuhne-electronic.com/kuhne/en/shop/amateur-radio/power-amplifiers/MKU+47+G2++Transverter/?card=1611>
5. <https://www.kuhne-electronic.com/funk/en/shop/industrial/prof-signal-sources/prof-oscillator/MKU+LO+813+PLL2++Oscillator/?card=1910>
6. A. Mlynek et al, A simple and versatile phase detector for heterodyne interferometers, *Review of Scientific Instruments* **88**, 023504 (2017); <https://doi.org/10.1063/1.4975992>
7. D. Aguiam et al, Implementation of the new multichannel X-mode edge density profile reflectometer for the ICRF antenna on ASDEX Upgrade, *Review of Scientific Instruments* **87**, 11E722 (2016); <https://doi.org/10.1063/1.4961558>
8. R. L. Ramey and T. S. Lewis, Properties of Thin Metal Films at Microwave Frequencies, *Journal of Applied Physics* **39**, 1747 (1968); <https://doi.org/10.1063/1.1656424>